*Journal of Sound and Vibration* (2003) **259**(1), 145–160
doi:10.1006/jsvi.2002.5132, available online at http://www.idealibrary.com on IDEAL®

# CRACK DETECTION IN BEAM-TYPE STRUCTURES USING FREQUENCY DATA

J.-T. Kim

*Department of Ocean Engineering, Pukyong National University, Nam-Gu, Pusan* 608-737, *Republic of Korea*

AND

N. Stubbs

*Department of Civil Engineering, Texas A&M University, College Station, TX* 77843, *U.S.A*

(*Received* 1 *May* 2001, *and in final form* 31 *January* 2002)

A practical method to non-destructively locate and estimate size of a crack by using changes in natural frequencies of a structure is presented. First, a crack detection algorithm to locate and size cracks in beam-type structures using a few natural frequencies is outlined. A crack location model and a crack size model are formulated by relating fractional changes in modal energy to changes in natural frequencies due to damage such as cracks or other geometrical changes. Next, the feasibility and practicality of the crack detection scheme are evaluated for several damage scenarios by locating and sizing cracks in test beams for which a few natural frequencies are available. By applying the approach to the test beams, it is observed that crack can be confidently located with a relatively small localization error. It is also observed that crack size can be estimated with a relatively small size error.



## 1. INTRODUCTION

During the past two decades, a significant amount of research has been conducted in the area of non-destructive damage evaluation (NDE) via changes in the dynamic modal responses of a structure. The NDE methods developed up to date can be classified into four levels [1]: (1) Level I Methods, i.e., those methods that only identify if damage has occurred [2, 3]; (2) Level II Methods, i.e., those methods that identify if damage has occurred and simultaneously determine the location of damage [4–6]; (3) Level III Methods, i.e., those methods that identify if damage has occurred, determine the location of damage as well as estimate the severity of damage [7–10]; and (4) Level IV Methods, i.e., those methods that identify if damage has occurred, determine the location of damage, estimate the severity of damage, and evaluate the impact of the damage on the structure. Despite these combined research efforts in Levels II and III methods, several problems remain to be solved before damage assessment in real structures becomes a routine activity. Among these problems, a need remains to develop practical theories of damage detection to simultaneously predict the location of damage and estimate the geometric size of damage (e.g., quantification of crack depths or corrosive zones) in structures. A need also remains to circumvent the reality of being capable of measuring only limited modal information.

0022-460X/02/$35.00 

The primary contribution this study aims to make is on the development of a preliminary diagnostics via monitoring changes in natural frequencies of structures. Natural frequency is one of the most common modal features that are used in crack detection in structures. The appealing feature is that the natural frequency is relatively simple to measure and apply for the further use to structures. Also, monitoring natural frequencies is time and cost efficient in most structures. Research studies to non-destructively detect crack location and magnitude via changes in natural frequencies have been performed by many researchers. Attempts have been made to relate changes in natural frequencies to changes in beam properties such as cracks, notches, or other geometrical changes [11–13] and to identify crack location and magnitude in a beam from vibration modes [4, 14–16]. The authors have worked on the topic in sensitivity approach [7]. In the sensitivity approach, damage in a structural element is estimated from a direct inverse solution of a change in the element stiffness if modal sensitivity is computed from an analytical model of the structure and changes in natural frequencies are measured from the structure. Even though the sensitivity approach can produce an estimation of location and severity of damage at the same time, reliable output may not be expected unless both the analytical model that should be accurate enough to compute the modal sensitivity and a large number of frequencies that should be accurately measured are provided, noting that even significant damage may cause very small changes in natural frequencies and these changes may go undetected due to measurement or processing errors.

In order to improve those difficulties, the authors have adopted the presented methodology in which crack localization is performed first using a crack location model and crack size estimation at the predicted location is performed thereafter using a crack size estimation model [11–13]. Also, the presented method uses only a few frequencies. The crack location model relates frequency ratios of a few measured modes to modal sensitivity ratio of the corresponding modes to identify potential crack locations [4, 17, 18]. For each predicted location, the crack size estimation model relates fractional changes in measured frequencies to a geometric crack size on the basis of the theory of the linear fracture mechanics.

In this paper, we present a practical methodology to non-destructively localize cracks and estimate the sizes of the cracks in beam-type structures using changes in frequencies. First, we outline a crack detection algorithm to locate and size cracks in beam-type structures using a few natural frequencies. A crack location model and a crack size estimation model are formulated by relating fractional changes in modal energy to changes in natural frequencies due to damage such as cracks or other geometrical changes. Next, we demonstrate the feasibility and practicality of the crack detection scheme by locating and sizing cracks in test beams. Finally, we assess the accuracy of the crack detection results obtained from test beams for which natural frequencies were measured for several damage scenarios [19].

## 2. CRACK DETECTION METHOD

The scheme shown in Figure 1 represents a crack detection method that yields information on location and geometrical size of damage directly from changes in modal characteristics of a target structure. The modal characteristics of interest here are natural frequencies. Once, two sets of natural frequencies are experimentally measured for the as-built structure and its corresponding damaged state, the crack detection methodology to be described here is used to predict crack locations and to estimate geometrical sizes of those predicted cracks. Note that system identification (SID) techniques can be adopted

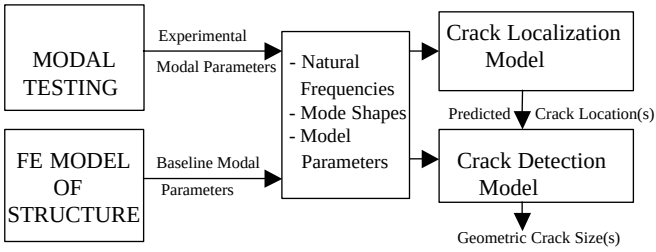


Figure 1. Non-destructive crack detection scheme.

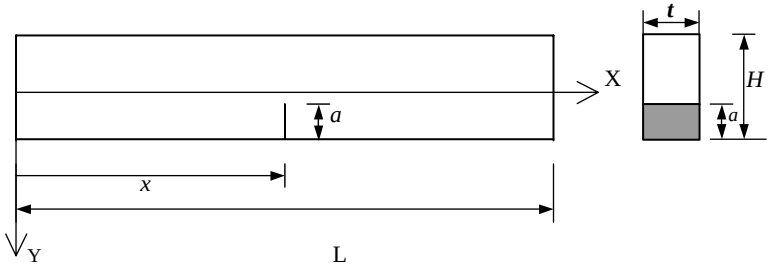


Figure 2. Geometry of free–free beam with a crack.

to generate baseline modal parameters if there are no field records on the reference structure [20].

### 2.1. CRACK-SIZE MODEL

With reference to Figure 2, suppose we are given an undisturbed (i.e., undamaged) *m-d.o.f.* structural system that yields the $i$th natural frequency $\omega_i$ and the $i$th mode shape $\phi_i$. Next, assume that at some later time the structure is damaged (i.e., geometrical changes due to the crack as shown in Figure 2) in one or more locations of the structure. The resulting characteristic equation of the damaged structure yields the $i$th natural frequency $\omega_i^*$ and the $i$th mode shape $\phi_i^*$. (Note that the asterisk characterizes the damaged structure.)

Assuming no volume changes due to cracks or other geometrical changes, Gudmunson [11] proposed a first order perturbation method that predicts the changes in natural frequencies of a structure resulting from the damage. For small cracks, the fractional changes in modal strain energy can be related to the fractional changes in frequency as follows:

$$\frac{\delta W_i}{W_i} = \frac{\delta \lambda_i}{\lambda_i}, \tag{1}$$

where $W_i$ is the $i$th modal strain energy of the initial structure, $\delta W_i$ is the loss in the $i$th modal strain energy after damage, and $\delta\lambda_i/\lambda_i$ is the fractional change in the $i$th eigenvalue due to the damage.

In the present study, we limit our discussion on the crack-size model to Euler–Bernoulli beams. If the Euler–Bernoulli beam theory is used, the $i$th modal strain energy $W_i$ can be

written as

$$W_i = \int_0^L \tfrac{1}{2} EI\{\phi_i''(x)\}^2 \, \mathrm{d}x, \tag{2}$$

where $E$ is Young's modulus, $I$ is the second moment of area, $L$ is the beam span length, and $\phi_i(x)$ is the $i$th mode shape function. Next, the strain energy for the crack problem can be computed from the energy release rate by implementing linear elastic fracture mechanics. On assigning plane strain condition to the cracked beam, the energy loss rate of the $i$th modal strain energy is given by [21]

$$\frac{\partial \delta W_i}{\partial a} = t\frac{(1-v^2)}{E} K_I^2, \tag{3}$$

where $\partial \delta W_i / \partial a_i$ is the energy loss rate of the $i$th modal strain energy with respect to crack depth, $t$ is the beam thickness, $v$ is the Poisson ratio, and $K_I$ is the stress intensity factor depending on crack depth $a$, applied flexural stress level $\sigma$, and beam dimension (e.g., thickness $t$, height $H$ and length $L$ as shown in Figure 1).

For the edge-crack case under bending motion (e.g., as shown in Figure 2), the stress intensity factor is given by

$$K_I = F \cdot \sigma\sqrt{\pi a}. \tag{4}$$

The term $F$ is a geometrical factor depending on dimensionless crack depth ratio $a/H$ [22, 23], where

$$F = 1{\cdot}122 - 1{\cdot}40(a/H) + 7{\cdot}33(a/H)^2 - 13{\cdot}08(a/H)^3 + 14{\cdot}0(a/H)^4. \tag{5}$$

Substituting equations (4) and (5) into equation (3) and further integrating equation (3) over the crack contour generates

$$\delta W_i = \left(\frac{\pi t(1-v^2)}{2E} F^2 \sigma_k^2 a_k^2\right)_i \tag{6}$$

in which, for the $i$th mode, $a_k = a(x_k)$ represents the crack size at location $x_k$ and $\sigma_k = \sigma(x_k)$ represents the maximum flexural stress at location $x_k$ along the beam's longitudinal axis. For the Euler–Bernoulli beam, the stress level is given by

$$\sigma(x_k) = \tfrac{1}{2} E\, H \phi_i''(x_k). \tag{7}$$

On dividing equation (6) by equation (2), the fractional change in the $i$th modal strain energy is given by

$$\frac{\delta W_i}{W_i} = \frac{\pi t(1-v^2)}{4}\frac{H^2}{I} F^2 S_{ik} a_k^2 \tag{8}$$

and

$$S_{ik} = \int_k \{\phi_i''\}^2 \, \mathrm{d}x \Big/ \int_0^L \{\phi_i''\}^2 \, \mathrm{d}x \tag{9}$$

in which $S_{ik}$ represents the sensitivity of the $k$th location in the $i$th modal strain energy.

On substituting equation (2)–(8) into equation (1), we obtain a relation between the crack depth and the fractional changes in the $i$th eigenvalue as follows:

$$\frac{\delta \lambda_i}{\lambda_i} = \eta S_{ik} \left(\frac{a_k}{H}\right)_i^2 \tag{10}$$

and for the beam section considered here:

$$\eta = 0.25\pi t(1-v^2) F^2 H^4 I^{-1} \tag{11}$$

in which $(a_k/H)_i$ is the dimensionless crack size at the $k$th location defined in the $i$th mode and $\eta$ is a constant value depending on beam dimensions, crack types, and the Poisson ratio. equation (10) can be solved to estimate crack sizes if the quantities $\delta\lambda_i/\lambda_i$ and $S_{ik}$ are experimentally determined or numerically generated.

### 2.2. CRACK-LOCATION MODEL

A crack-location model is formulated from linearly relating the structural system's sensitivity on modal characteristics to the eigenfrequency changes due to geometrical changes as described in Figure 2. For an *m-d.o.f.* structural system of $NE$ elements and $N$ nodes, the damage inflicted at predefined locations may be predicted using the following sensitivity equation [7]:

$$\sum_{j=1}^{NE} F_{ij}\alpha_j = Z_i \tag{12}$$

in which $\alpha_j$ $(-1 \leq \alpha_j \leq 0)$ is the damage inflicted at the $j$th location (i.e., the fractional reduction in $j$th stiffness parameter). The term $Z_i$ is the fractional change in the $i$th eigenvalue and (by neglecting changes in mass due to damage) is given by

$$Z_i = \delta\omega_i^2/\omega_i^2, \tag{13}$$

where $\delta\omega_i^2 (= \omega_i^{*2} - \omega_i^2)$ is the change in the $i$th damped natural frequency before and after damage. The term $F_{ij}$ is the modal sensitivity of the $i$th modal stiffness with respect to the $j$th element.

$$F_{ij} = K_{ij}/K_i, \tag{14}$$

where $K_i$ is the $i$th modal stiffness ($K_i = \Phi_i^{\mathrm{T}}\mathbf{C}\Phi_i$) and $K_{ij}$ is the contribution of the $j$th element to the $i$th modal stiffness ($K_{ij} = \Phi_i^{\mathrm{T}}\mathbf{C}_j\Phi_i$). Also, $\Phi_i$ is the $i$th modal vector, $\mathbf{C}$ is the system stiffness matrix, and $\mathbf{C}_j$ is the contribution of $j$th element to the system stiffness.

Once the quantity $Z_i$ is experimentally determined, equation (12) can be solved to locate and size damage in the system. However, the inverse solution is possible only if the number of damage parameters is close to the number of modes (i.e., $NE \approx NM$) [20]. In the case when $NE \gg NM$, the system becomes ill-conditioned and alternate methods to estimate damage parameters should be sought. In an effort to overcome this difficulty, Stubbs *et al.* [17] proposed a sensitivity ratio concept based on earlier works presented by Cawley and Adams [4].

Let us consider the structural system of $NE$ elements ($j = 1, 2, \ldots, q, \ldots, NE$) and a measured set of $NM$ vibration modes ($i = 1, \ldots, m, n, \ldots, NM$). Equation (12) is rewritten for any two modes $m$ and $n$ ($m \neq n$) respectively. On dividing equation (12) for mode $m$ by the other for mode $n$, we obtain

$$\frac{Z_m}{Z_n} = \frac{\sum_{j=1}^{NE} F_{mj}\alpha_j}{\sum_{j=1}^{NE} F_{nj}\alpha_j} = \frac{F_{m1}\alpha_1 + F_{m2}\alpha_2 + \cdots + F_{mq}\alpha_q + \cdots + F_{mNE}\alpha_{NE}}{F_{n1}\alpha_1 + F_{n2}\alpha_2 + \cdots + F_{nq}\alpha_q + \cdots + F_{nNE}\alpha_{NE}}. \tag{15}$$

Assuming that the structure is damaged in a single element, such that $\alpha_j \neq 0$ when $j = q$ but $\alpha_j = 0$ when $j \neq q$, equation (15) is rewritten by

$$\frac{Z_m}{Z_n} = \frac{F_{mq}}{F_{nq}} \tag{16}$$

in which $Z_m/Z_n$ is the measured ratio of the fractional changes in frequency for two modes, $m$ and $n$. Also, $F_{mq}/F_{nq}$ is the ratio of the theoretically measured sensitivities for

those modes and the element $q$. So the damage inflicted at that location is defined using equation (16) when the LHS equals to the RHS.

For all measured $NM$ modes, equation (16) can be extended into

$$\frac{Z_m}{\sum_{k=1}^{NM} Z_k} = \frac{F_{mq}}{\sum_{k=1}^{NM} F_{kq}}. \tag{17}$$

Since equation (17) is true only if element $q$ is damaged, we introduce an error index into equation (17) as follows:

$$e_{ij} = \frac{Z_m}{\sum_{k=1}^{NM} Z_k} - \frac{F_{mq}}{\sum_{k=1}^{NM} F_{kq}}, \tag{18}$$

where $e_{ij}$ represents localization error for the $i$th mode and the $j$th location, and $e_{ij} = 0$ indicates that the damage is located at $j$th location using the $i$th modal information. To account for all available modes we form a single damage indicator (DI) for the $j$th member as

$$DI_j = \left[\sum_{i=1}^{NM} e_{ij}^2\right]^{-1/2}, \tag{19}$$

where $0 \leqslant DI_j < \infty$ and the damage is located at element $j$ if $DI_j$ approaches the local maximum point. In principle, the proposed method works if at least two modes are given. But it is important to notice that the accuracy of damage identification is up to either the number of modes or the type of modes that are used in the process.

## 3. EXPERIMENTAL VERIFICATION

### 3.1. DESCRIPTION OF TEST STRUCTURE

The crack detection model will be validated using a comprehensive data provided by Silva and Gomes [19]. Those researchers performed an extensive set of modal analysis experiments on free–free uniform beams with the goal of providing objective data to validate proposed techniques for damage detection. Test specimens were steel beams with $0{\cdot}032\,\text{m} \times 0{\cdot}016\,\text{m}$ rectangular cross-section and $0{\cdot}72\,\text{m}$ long. The corresponding material properties were: $E = 206\,\text{GPa}$, $\upsilon = 0{\cdot}29$, and $\rho = 7650\,\text{kg/m}^3$.

Here the results of 32 experiments reported by Silva and Gomes [19] are utilized: 16 experiments on undamaged beams and corresponding 16 experiments on damaged beams. The following procedures were utilized for the experiments. The first four bending frequencies were measured for each of 16 undamaged free–free beams. Then a cut was introduced into each beam and the same four bending frequencies were measured. The crack in each beam was simulated by a cut normal to the beams' longitudinal axis, with a controlled depth (as listed in Table 1). The thickness of the cut was carefully defined taking into account that both sides of the crack were not supposed to make contact during the dynamic bending of the beam.

Table 1 presents the total 16 damage scenarios that include four different crack-locations and four crack-depth levels at each location. The two sets of bending frequencies measured before and after the damage episodes are listed in Table 1.

TABLE 1

*Damage scenarios and resonance frequencies (Hz) of free–free beams [19]*

| Crack case | Inflicted crack | | Mode 1 | | Mode 2 | | Mode 3 | | Mode 4 | |
|---|---|---|---|---|---|---|---|---|---|---|
| | Location $(x/L)$ | Size $(a/H)$ | Initial | Cracked | Initial | Cracked | Initial | Cracked | Initial | Cracked |
| 1 | 0·125 | 0·125 | 315·9 | 316·0 | 860·2 | 859·4 | 1654·5 | 1649·0 | 2668·0 | 2653·0 |
| 2 | 0·125 | 0·25 | 316·3 | 316·1 | 862·6 | 857·8 | 1659·0 | 1632·5 | 2674·0 | 2608·0 |
| 3 | 0·125 | 0·375 | 317·6 | 316·6 | 864·6 | 851·4 | 1663·0 | 1593·5 | 2682·0 | 2520·0 |
| 4 | 0·125 | 0·5 | 314·7 | 313·0 | 856·8 | 826·6 | 1647·0 | 1515·0 | 2657·0 | 2378·0 |
| 5 | 0·25 | 0·125 | 316·8 | 315·9 | 861·6 | 855·2 | 1657·5 | 1647·5 | 2673·0 | 2665·0 |
| 6 | 0·25 | 0·25 | 317·7 | 314·1 | 864·4 | 840·6 | 1662·0 | 1626·5 | 2676·0 | 2666·0 |
| 7 | 0·25 | 0·375 | 317·8 | 308·8 | 864·8 | 805·2 | 1662·5 | 1580·5 | 2675·0 | 2660·0 |
| 8 | 0·25 | 0·5 | 323·8 | 305·4 | 878·8 | 870·4 | 1689·5 | 1534·0 | 2721·0 | 2685·0 |
| 9 | 0·375 | 0·125 | 313·5 | 311·7 | 855·0 | 853·8 | 1646·0 | 1646·5 | 2657·0 | 2652·0 |
| 10 | 0·375 | 0·25 | 315·4 | 307·1 | 858·6 | 842·4 | 1653·0 | 1651·5 | 2665·0 | 2604·0 |
| 11 | 0·375 | 0·375 | 316·6 | 296·2 | 862·4 | 825·0 | 1659·5 | 1655·5 | 2675·0 | 2532·0 |
| 12 | 0·375 | 0·5 | 328·8 | 279·0 | 873·4 | 805·2 | 1679·5 | 1672·0 | 2707·0 | 2439·0 |
| 13 | 0·5 | 0·125 | 316·7 | 313·0 | 862·8 | 863·2 | 1658·0 | 1645·5 | 2675·0 | 2676·0 |
| 14 | 0·5 | 0·25 | 315·6 | 303·0 | 859·4 | 859·8 | 1652·0 | 1606·5 | 2667·0 | 2665·0 |
| 15 | 0·5 | 0·375 | 317·8 | 291·5 | 865·8 | 866·0 | 1664·5 | 1574·0 | 2687·0 | 2683·0 |
| 16 | 0·5 | 0·5 | 320·6 | 265·1 | 873·0 | 873·2 | 1678·0 | 1498·0 | 2701·0 | 2701·0 |

TABLE 2

*Comparison of frequency: undamaged beams versus baseline model*

| Mode no. | Average frequency of 16 uncracked beams | Frequency from modal analysis | Coefficient of variation |
|---|---|---|---|
| 1 | 317·85 | 318·07 | 0·010 |
| 2 | 864·01 | 863·02 | 0·008 |
| 3 | 1661·59 | 1657·96 | 0·008 |
| 4 | 2678·75 | 2675·75 | 0·006 |

### 3.2. CRACK DETECTION PRACTICE

The Euler–Bernoulli beam model was selected as the mathematical representation for crack detection practice. For analysis purposes we divided the 72 cm beam into 72 elements of equal size. Each element is a potential damage location and has a spacing of 1 cm or 1·38 per cent (i.e., $\frac{1}{72} \times 100$) of the beam span. Crack detection practice on the model was performed in five steps.

In the first step, theoretical modal analysis was performed and a system identification technique proposed by Kim and Stubbs [10] was used to identify baseline modal parameters of the beam. The average frequencies of the 16 undamaged beams and the generated frequencies of an identified baseline model are compared as listed in Table 2. Note that the coefficients of variation (COVs) are less than 0·01 for all modes.

In the second step, the modal sensitivity (i.e., the equivalent expression of equation (14)) of mode $i$ and element $j$ between two locations $(x_j, x_{j+1})$ was computed using

$$F_{ij} = \int_{x_j}^{x_{j+1}} EI\{\phi_i''(x)\}^2 \frac{\mathrm{d}x}{K_i}, \qquad K_i = \int_0^l EI\{\phi_i''(x)\}^2 \,\mathrm{d}x. \tag{20}$$

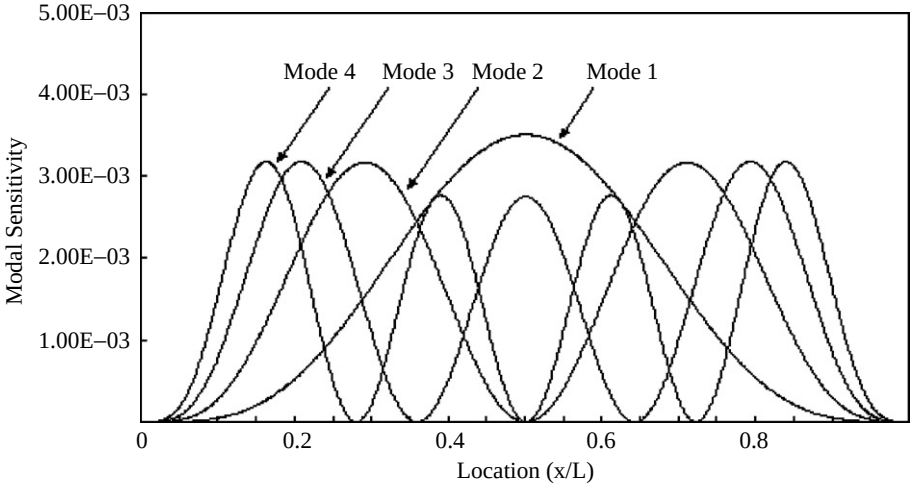


Figure 3. Modal sensitivities of free–free beam.

The flexural rigidity $EI$ is assumed constant over the beam span. The curvatures of the mode shapes were generated at the 73 nodes of the DDM. The curvatures were obtained as follows: (1) modal amplitudes corresponding to nodes 1–73 were generated from theoretical modal analysis; (2) a modal displacement function $w(x)$ was generated for the entire beam using a third order interpolation function; and (3) the curvatures (i.e., $\phi''(x)$) were determined at the 73 nodes. Since four measured frequencies are available, the sensitivities are defined for four modes and 72 elements. Figure 3 shows the modal sensitivities of the test beam that were computed along the beam's longitudinal axis.

In the third step, we predicted potential crack locations. We computed the fractional changes in frequencies (i.e., equation (15)) using the measured frequency results listed in Table 1. By assuming that $EI$ is constant over the beam span, the sensitivity ratio (i.e., the RHS of equation (17)) for an element $q$ and for any two modes $m$ and $n$ can be rewritten by

$$\frac{F_{mq}}{F_{nq}} = \frac{\int_q \{\phi_m''\}^2 \, \mathrm{d}x}{\int_q \{\phi_n''\}^2 \, \mathrm{d}x} \frac{\int_0^l \{\phi_n''(x)\}^2 \, \mathrm{d}x}{\int_0^l \{\phi_m''(x)\}^2 \, \mathrm{d}x}. \tag{21}$$

Next, we computed localization errors using equation (18) for four modes and 72 locations (i.e., $e_{1j}$, $e_{2j}$, $e_{3j}$, and $e_{4j}$, $j = 1, 72$) by implementing the sensitivity ratios and the fractional changes in frequencies. For example, error indices are plotted in Figures 4–7 for the following four cases: Crack Case 2 ($a/h = 0{\cdot}125$ and $x/L = 0{\cdot}25$), Crack Case 6 ($a/h = 0{\cdot}125$ and $x/L = 0{\cdot}25$), Crack Case 10 ($a/h = 0{\cdot}125$ and $x/L = 0{\cdot}375$), and Crack Case 14 ($a/h = 0{\cdot}125$ and $x/L = 0{\cdot}5$). Note for each case along the $x$ co-ordinate that each point where error equals to zero indicates that a crack is located at that location. Finally, we computed the damage index (i.e., given by equation (19)) to decide potential crack locations. Damage indices are plotted in Figures 8–11 for Crack Cases 2, 6, 10, and 14 respectively. Note for each crack case that because of symmetry two predictions are made thus one location is false-alarmed. The crack localization results for all the 16 damage cases are summarized in Table 3.

In the fourth step, crack size at each predicted location was estimated by using the crack size model (i.e., the equivalent expression of equation (10)). Assuming a crack is located in

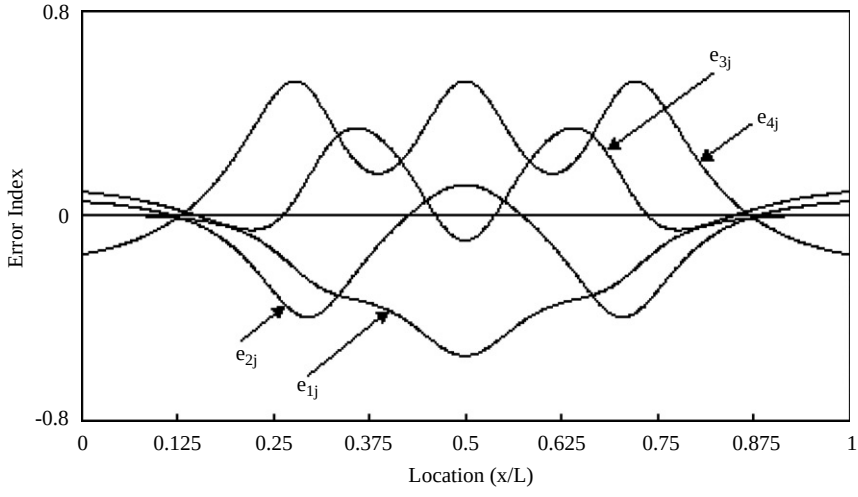


Figure 4. Localization error indices for individual modes for Crack Case 2.

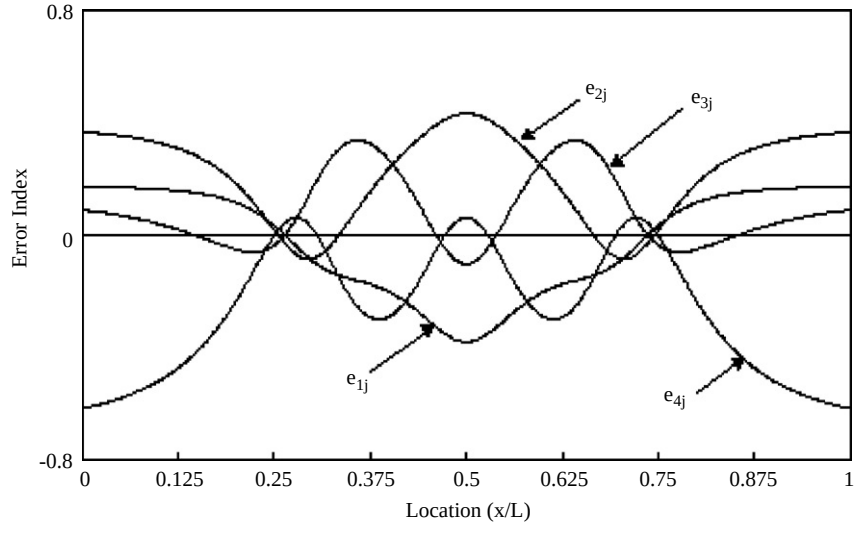


Figure 5. Localization error indices for individual modes for Crack Case 6.

element $j$ between two locations $(x_j, x_{j+1})$, a solution of crack size is given by

$$\left(\frac{a_k}{H}\right)_i = \sqrt{\frac{\delta\lambda_i}{\eta S_{ik}\lambda_i}}, \tag{22}$$

where $(a_k/H)_i$ is the dimensionless crack size estimated at location $x_k(=(x_j + x_{j+1})/2)$ by using the $i$th modal data. As stated previously, the vertical crack-depth of opening fracture mode is our primary attention. The modal sensitivity of mode $i$ and location $k$ was computed using equation (20). The constant $\eta$ was obtained from equation (11) by implementing $H = 0{\cdot}032$ m, $L = 0{\cdot}72$ m, the Poisson ratio of 0·29, and the geometrical factor $F = 1{\cdot}12$ (i.e., an approximate value of equation (5) for a small edge-crack). The

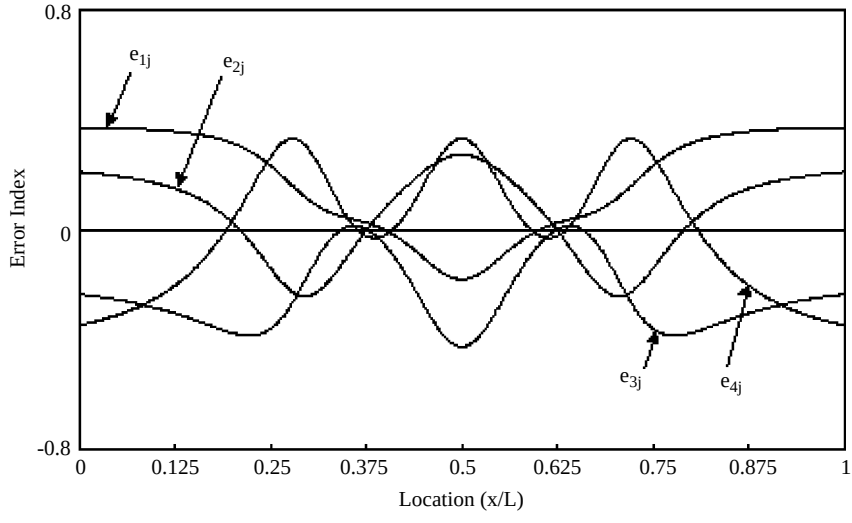


Figure 6. Localization error indices for individual modes for Crack Case 10.

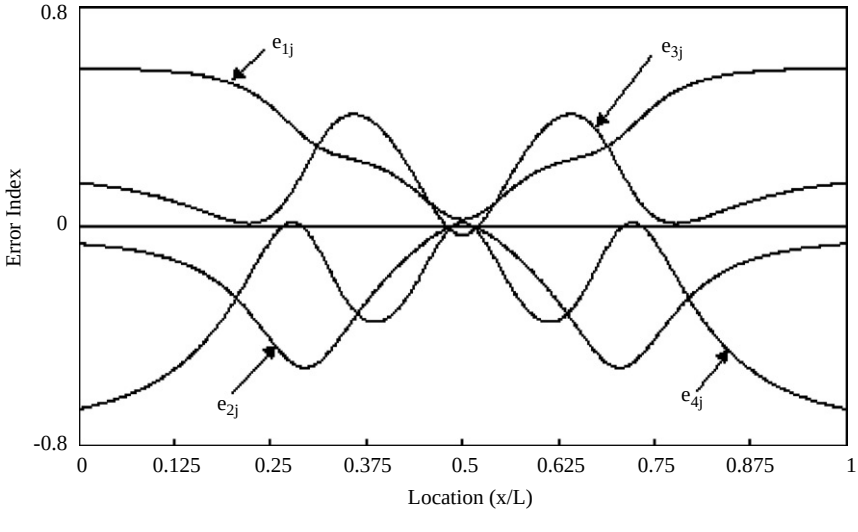


Figure 7. Localization error indices for individual modes for Crack Case 14.

fractional changes in the eigenvalues were computed from equation (15) by implementing the measured frequencies listed in Table 1. The crack sizing results for the 16 damage cases are summarized in Table 2.

### 3.3. *Assessment of crack detection results*

From the analysis it is observed that at least three modes are needed to detect damage existing anywhere in the beam. Individual modes have relatively different sensitivities to potential damage locations in the beam (as shown in Figure 3). For example, modes 1 and 3 are sensitive to the locations near the center while modes 2 and 4 are not sensitive (i.e.,

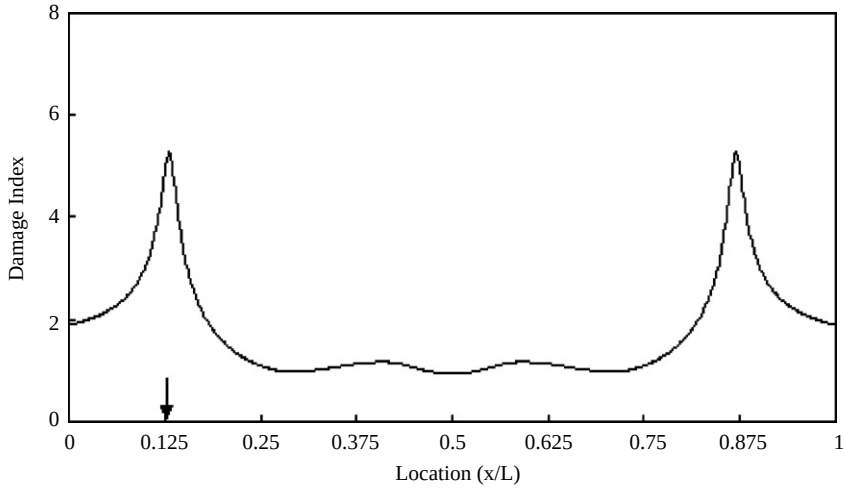


Figure 8. Crack localization results of Crack Case 2.

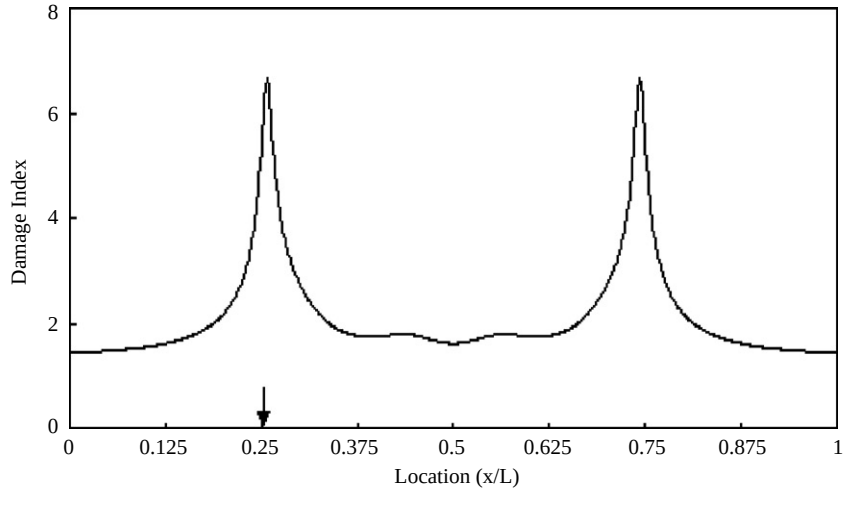


Figure 9. Crack localization results of Crack Case 6.

zero sensitivity at the center). Therefore, if damage presents near the center, a good prediction can be expected if the two modes modes 1 and 3 are used or if a series of modes including modes 1 or 3 are used. In this study, Figures 4–11 illustrate that the accuracy of crack localization can be improved as more modes are used in the process since localization errors are decreased by averaging results of individual modes.

The accuracy of the crack localization scheme presented here is evaluated by measuring the so-called localization error. The localization error *le*, which represents the metrical difference between real crack location and predicted location, is quantified using the expression

$$le = (\Delta x/L) \times 100 \tag{23}$$

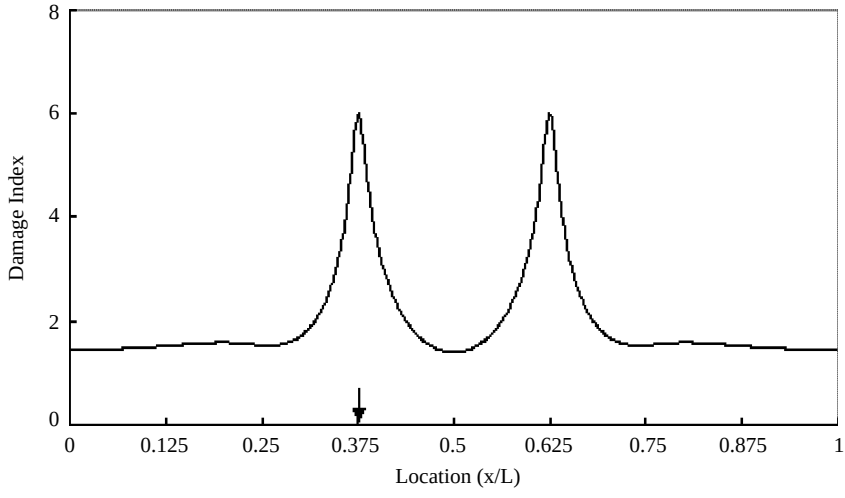


Figure 10. Crack localization results of Crack Case 10.

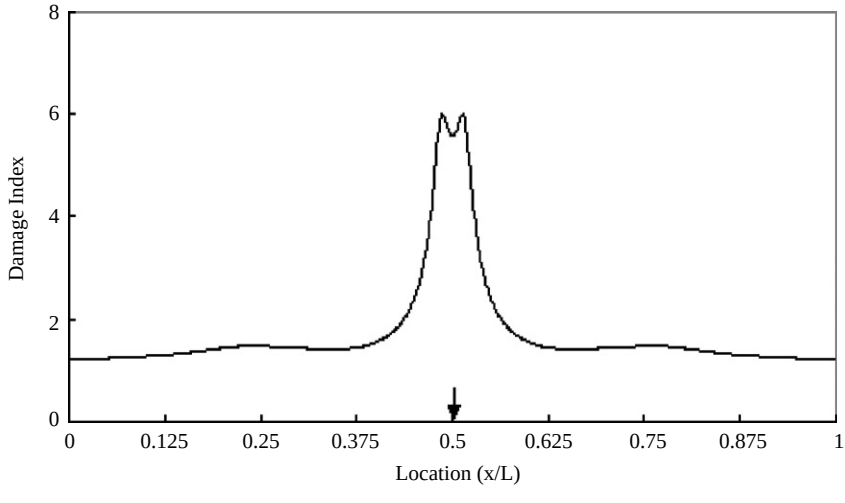


Figure 11. Crack localization results of Crack Case 14.

in which *le* is the spacing between the inflicted and predicted location and $L$ is the reference span. A comparison between the inflicted and predicted locations of crack is plotted in Figure 12. The location error was computed by equation (23) and the results are summarized in Table 3. The minimum location error is 0·1 per cent. It means that the predicted location falls within less than 0·1 cm of the correct location in the test beam (note that $L = 72$ cm). The maximum location error is 4·8 per cent (damage case 16) and it means 3·4 cm away from the correct location in the test beam. The average location error is 1·3 per cent. By excluding Damage Case 16 that exceeds two standard deviations, localization errors range in 0·1–2·1 per cent.

The accuracy of the crack sizing scheme presented here is evaluated by measuring the so-called size error. The size error *se*, which represents the difference between real and

TABLE 3

*Crack prediction and accuracy assessment results of test beams*

| Crack case | Inflicted crack(*s*) | | Predicted crack(*s*) | | Prediction accuracy | |
|---|---|---|---|---|---|---|
| | Location $(x/L)$ | Size $(a/H)$ | Location $(x/L)$ | Size $(a/H)$ | Loc. error % | Sizing error (%) |
| 1 | 0·125 | 0·125 | 0·110 | 0·126 | 1·5 | 1·1 |
| 2 | 0·125 | 0·25 | 0·121 | 0·234 | 0·4 | 6·0 |
| 3 | 0·125 | 0·375 | 0·140 | 0·335 | 1·5 | 10·4 |
| 4 | 0·125 | 0·5 | 0·146 | 0·440 | 2·1 | 11·8 |
| 5 | 0·25 | 0·125 | 0·243 | 0·131 | 0·7 | 5·1 |
| 6 | 0·25 | 0·25 | 0·257 | 0·244 | 0·7 | 2·2 |
| 7 | 0·25 | 0·375 | 0·264 | 0·395 | 1·4 | 5·5 |
| 8 | 0·25 | 0·5 | 0·256 | 0·434 | 0·6 | 13·1 |
| 9 | 0·375 | 0·125 | 0·326 | 0·093 | 4·8 | 25·4 |
| 10 | 0·375 | 0·25 | 0·376 | 0·226 | 0·1 | 9·3 |
| 11 | 0·375 | 0·375 | 0·378 | 0·345 | 0·3 | 7·9 |
| 12 | 0·375 | 0·5 | 0·390 | 0·439 | 1·5 | 12·1 |
| 13 | 0·5 | 0·125 | 0·511 | 0·132 | 1·1 | 6·0 |
| 14 | 0·5 | 0·25 | 0·514 | 0·232 | 1·4 | 6·8 |
| 15 | 0·5 | 0·375 | 0·486 | 0·328 | 1·4 | 12·4 |
| 16 | 0·5 | 0·5 | 0·511 | 0·488 | 1·1 | 2·3 |

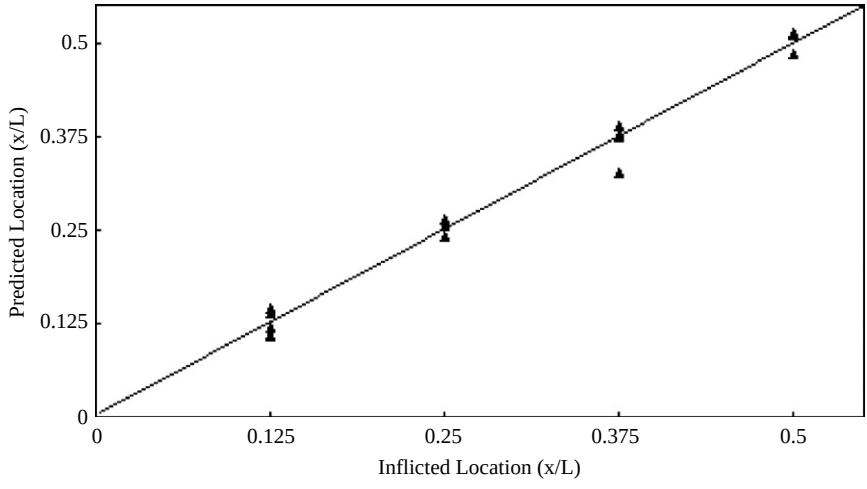


Figure 12. Comparison of inflicted crack location and predicted crack location.

predicted crack depth, is quantified using the expression

$$se = |\{(a/H)_r - (a/H)_p\}/(a/H)_r| \tag{24}$$

in which $(a/H)_r$ is the inflicted real crack-depth and $(a/H)_p$ is the predicted crack-depth. The size error was evaluated using equation (24). A comparison between the inflicted and predicted crack sizes is plotted in Figure 13 and the results are also summarized in Table 3. The size errors range in 1·1–24·4 per cent. For example, per cent error means 0·1 mm difference in the estimation of 10-mm crack depth. The average size-error is 8·6 per cent.

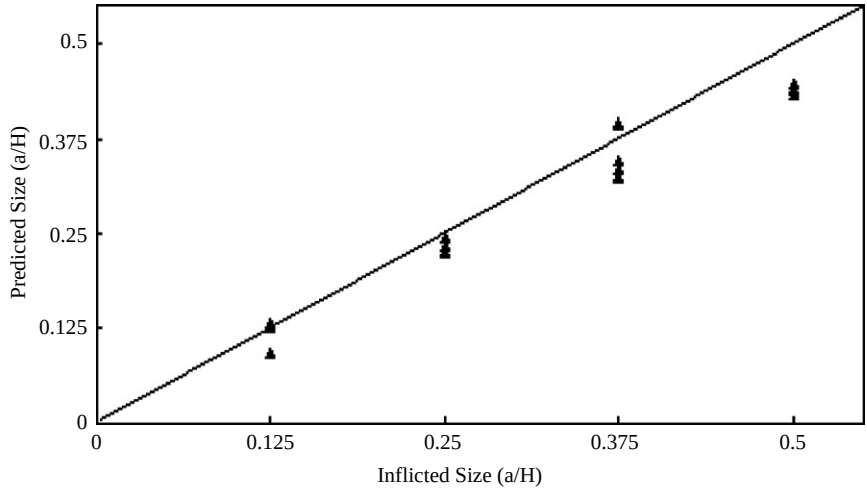


Figure 13. Comparison of inflicted crack depth and predicted crack depth.

By excluding Damage Case 16 that exceeds two standard deviations, size errors range in 1·1–13·1 per cent.

In theory, the presented method may detect any crack sizes that cause changes in beam's stiffness and result in changes in natural frequencies. However, in reality, even a big crack might be remained undetected due to measurement and modelling uncertainties. For example, the effect of inconsistent measuring temperatures may cancel monitoring changes in natural frequencies in real structures. In this study, we use a set of deterministic test results reported by Silva and Gomez [19]. It is reported that the beams were tested under a controlled laboratory environment. Due to the same reasons, the effect of measurement errors on the accuracy of crack detection has not been examined here; however, the discussion on the problem should be expanded to quantify the effect of uncertainties due to measurement errors and environmental conditions on the accuracy of crack detection in beam structures. Previous studies on the topic by the authors are available as references [17, 10].

## 4. SUMMARY AND CONCLUSIONS

This paper presented a methodology to non-destructively locate and estimate size of crack in structures for which only a few natural frequencies are available. The proposed methodology was presented in two parts. The first part of the paper outlined a theory of crack detection that yielded information on the location and size of crack directly from changes in frequencies of the structures. A crack location model and a crack size estimation model were formulated by relating fractional changes in modal energy to changes in natural frequencies. The second part of the paper demonstrated the feasibility and practicality of the crack detection scheme by accurately locating and sizing cracks in test beams for which four natural frequencies were available for several damage scenarios.

By applying the approach to the test beam, it was observed that the crack can be confidently located with a relatively small localization error. It is also observed that the size of crack can be estimated with a relatively small size error. We conclude that it is

possible to localize a crack and estimate the crack size in a beam-type structure with knowledge of natural frequencies of only a few natural frequencies measured before and after damage.

Research to improve the crack detection algorithm presented is continuing along four lines of inquires. First, we are developing algorithms to more accurately detect the location and estimate the size of damage. Second, we need to assess the effect of uncertainties due to measurement errors and environmental conditions on the accuracy of the crack detection approach for beam structures. Third, we need to demonstrate the applicability of the method to several types of multiple cracks. The application of the method is not limited for detecting multiple cracks in beams, even though the presented method was derived assuming a beam damaged in a single location. However, the accuracy of detection may be lower than when applied for the single-crack cases. Fourth, we are now in advanced stages of demonstrating the effectiveness and practicality of the approach for laboratory-scale models and full-scale structures.

## ACKNOWLEDGMENTS

This study was supported by Korea Science and Engineering Foundation (KOSEF) through Smart Infra-Structure Technology Center in the program year of 2002.

## REFERENCES

1. A. Rytter 1993 *Ph.D. Dissertation, University of Aalborg, Denmark*. Vibration based inspection of civil engineering.
2. J. K. Vandiver 1975 *Proceedings of the 7th Annual Offshore Technology Conference, Houston, TX*, *Paper* 2267. Detection of structural failures on fixed platforms by measurement of dynamic responses.
3. H. Crohas and P. Lepert 1982 *Oil and Gas Journal*, **80**, 94–103. Damage detection monitoring method for offshore platforms is field tested.
4. P. Cawley and R. D. Adams 1979 *Journal of Strain Analysis* **14**, 49–57. The location of defects in structures from measurements of natural frequencies.
5. A. K. Pandey, M. Biswas and M. M. Samman 1991 *Journal of Sound and Vibration* **145**, 321–332. Damage detection from changes in curvature mode shapes.
6. J. Chance, G. R. Tomlinson and K. Worden 1994 *Proceedings of the 12th International Modal Analysis Conference, Honolulu, HI*, Vol. 1, 778–785. A simplified approach to the numerical and experimental modeling of the dynamics of a cracked beam.
7. N. Stubbs and R. Osegueda 1990 *International Journal of Analytical and Experimental Modal Analysis* **5**, 67–79. Global nondestructive damage evaluation in solids.
8. X. Wu, J. Ghaboussi and J. H. Garrett 1992 *Computers and Structures* **42**, 649–659. Use of neural networks in detection of structural damage.
9. M. Kaouk and D. C. Zimmerman 1994 *American Institute of Aeronautics and Astronautics Journal* **32**, 836–842. Structural damage assessment using a generalized minimum rank perturbation theory.
10. J. T. Kim and N. Stubbs 1995 *American Society of Civil Engineers Journal of Structural Engineering* **121**, 1409–1417. Model uncertainty and damage detection accuracy in plate-girder bridges.
11. P. Gudmunson 1982 *Journal of Mechanics and Physics of Solids* **30**, 339–353. Eigenfrequency changes of structures due to cracks, notches or other geometrical changes.
12. S. Cristides and A. D. S. Barrs 1984 *American Institute of Aeronautics and Astronautics Journal* **26**, 1119–1126. On-orbit damage assesment for large space structures.
13. P. F. Ricos, N. Aspragathos and A. D. Dimarogonas 1990 *Journal of Sound and Vibration* **138**, 381–388. Identification of crack location and magnitude in a cantilever beam from the vibration modes.

14. W. M. Ostachowicz and M. Krawczuk 1990 *Computers and Structures* **36**, 245–250. Vibration analysis of a cracked beam.
15. J. N. Sundermeyer and R. L. Weaver 1993 *TAM Report No*. 74, *UILU-ENG*-93–604, University of Illinois. On crack identification and characterization in a beam by nonlinear vibration analysis.
16. J. T. Kim, Y. S. Ryu and N. Stubbs 1998 *Fifth Pacific Structural Steel Conference, Seoul, Korea*, 1205–1210. Experimental verification of crack detection model using dynamic modal characteristics in structures.
17. N. Stubbs, J. T. Kim and K. Topole 1991 *Computational Stochastic Mechanics* (P. D. Spanos and C.A. Brebbia, editors), pp. 125–136. London: Elsevier Applied Science. The effect of model uncertainty on the accuracy of global nondestructive damage detection in structures.
18. J. M. Silva and A. J. L. Gomes 1994 *12th International Modal Analysis Conference, Honolulu, HI*, 1728–1735. Crack identification of simple structural elements through the use of natural frequency variations: the inverse problem.
19. J. M. Silva and A. J. L. Gomes 1990 *Experimental Mechanics* **20**, 20–25. Experimental dynamic analysis of cracked free–free beams.
20. N. Stubbs and J. T. Kim 1996 *American Institute of Aeronautics and Astronautics Journal* **34**, 1644–1649. Damage localization in structures without baseline modal parameters.
21. T. L. Anderson 1995 *Fracture Mechanics*. London: CRC Press.
22. J. M. Barsom and S. T. Rolfe 1999 *Fracture and Fatigue Control in Structures: Applications of Fracture Mechanics*. West Conshohoken, PA: Prentice Hall.
23. G. Gounaris and A. D. Dimarogonas, 1988 *Computers and Structures* **28**, 309–313. A finite element of a cracked prismatic beam for structural analysis.